Novel "Flow Injection" Channel Flow Cell for the Investigation of Processes at Solid/Liquid Interfaces. 2. Experiment

J. Justin Gooding,[†] Colin M. Brennan,[‡] John H. Atherton,[‡] Barry A. Coles,[†] and Richard G. Compton*,[†]

Physical and Theoretical Chemistry Laboratory, Oxford University, South Parks Road, Oxford OX1 3QZ, U.K., and Zeneca Limited, P.O. Box 42, Blackley, Manchester M9 3DA, U.K.

Received: April 5, 1996; In Final Form: July 25, 1996[⊗]

A novel "flow injection" channel flow cell, which enables the study of transient phenomena at diverse solid/liquid interfaces, is described. The cell is comprised of a rectangular duct through which solution flows under laminar flow conditions. In one wall of the duct is embedded the solid substrate of interest, and directly adjacent to this is the detector electrode. The solution species of interest enters the primary channel flow system from a secondary flow upstream of the solid substrate, located in the opposite wall, without seriously disrupting the well-defined flow profile in the former. The amount of the species injected, and the extent of any reaction with the solid substrate, is determined at the downstream detector electrode. Thus, the flow injection channel flow cell is similar to a double channel electrode but where the injection slit performs the function of the generator electrode (introducing a reactant species into the channel at a precise time). The rise time of the transient was comparable to a double channel electrode of analogous geometry (in which the generator electrode mimics the injection slit), and the detector current dies away to zero almost instantly once the injection is turned off. The variation in steady-state current with flow rate was shown to agree excellently with a theoretical description of the cell[1] without the need for any adjustable parameters. The cell was successfully used to monitor the reaction between the dye orange G and virgin cotton cloth.

Introduction

The channel flow cell has had considerable success in studying heterogeneous reactions at nonconducting solid/liquid interfaces.[2−6] The one limitation of the channel flow cell approach, however, is that it is restricted to steady-state measurements, and thus, some rapid reactions are excluded from investigation. To rectify this restriction, we have developed the "flow injection" channel flow cell for the investigation of rapid reactions between a solid substrate and a solution species under transient conditions. The concept of the flow injection channel flow cell was introduced in the previous theoretical publication.[1] This paper describes the experimental development of the successful flow injection cell. The flow system has two flow streams. One is the same as a conventional channel flow cell system through which flows the carrier solution. The injection solution flows through the second stream and enters the cell via a slit in the channel unit (Figure 1a). The reactant must diffuse across the channel to react with the solid substrate, embedded in the opposite wall of the channel, to be monitored by a detector electrode positioned downstream of the solid. The amount of reactant that reaches the solid is controlled by the carrier solution flow rate. In this format both transient and steady-state measurements can be conducted with the same flow cell and cell geometry.

The behavior of the flow injection cell is characterized with a model electrochemical system, the reduction of aqueous ferricyanide, and the variation of steady-state current with flow rate is compared to the values predicted using the FLOTRAN[7] and backward implicit finite difference[8−10] models outlined elsewhere.[1] The potential for this novel flow injection channel flow cell for investigating rapid reactions at solid/solution interfaces is illustrated by investigating the reaction between the model dye, orange G, and a cotton cloth. This dyeing reaction has been previously studied using a conventional channel flow cell.[2]

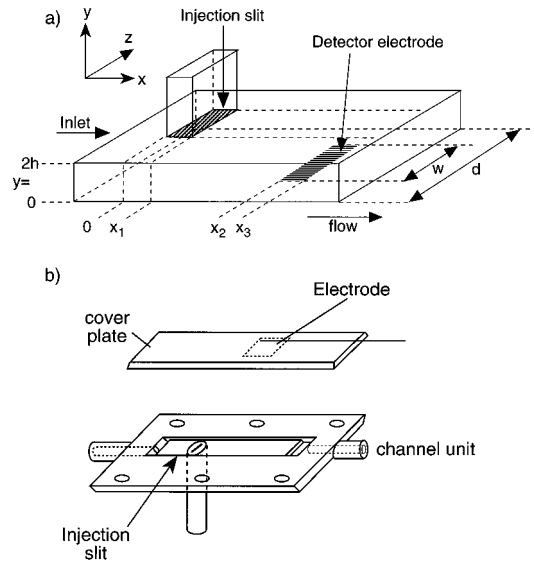

Figure 1. (a) Schematic of the flow injection channel flow cell with the coordinate system defined. (b) Flow injection channel flow cell.

Experimental Section

The flow injection channel flow cell is based on the principle of two flows entering the channel cell upstream of the detector electrode. The twin flow system is shown schematically in Figure 2. The reactant is contained in the secondary flow stream with a carrier solution in the primary flow stream. The flow rate in the carrier streams is controlled by the use of fine glass capillaries of different bore sizes and by varying the head

* To whom correspondence should be addressed.
† Oxford University.
‡ Zeneca Limited.
⊗ Abstract published in *Advance ACS Abstracts,* November 15, 1996.

S1089-5647(96)01035-8 CCC: $14.00

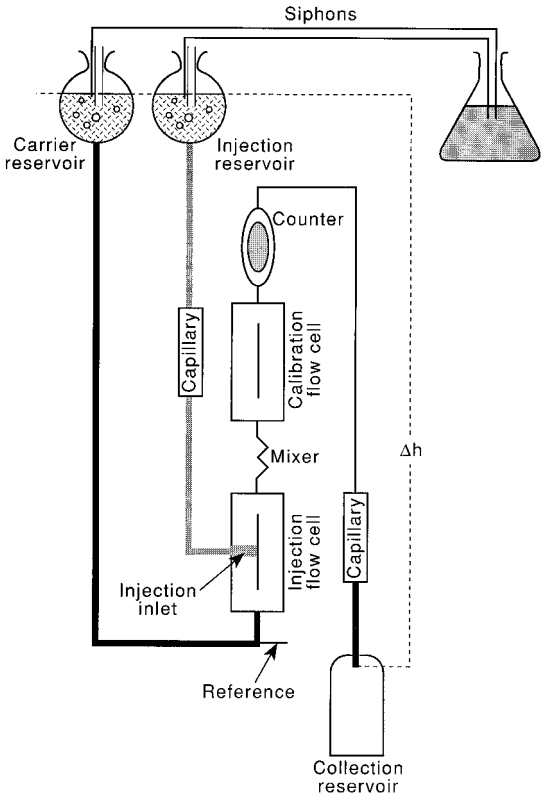

Figure 2. Flow system for the flow injection channel flow cell.

pressure, Δh, between the reservoir containing the carrier solution (the carrier reservoir) and the collection vessel at the exit of the flow system. This part of the flow system is the same as a conventional channel flow system. The injection solution flows from a reservoir (the injection reservoir) into the cell via a small slit. The injection secondary flow line is comprised of a long capillary of significantly finer bore than the smallest capillary used to control the main flow (Figure 2).

The carrier and injection reservoirs are set at the same height above the collection vessel, Δh, to allow injection solution to seep slowly into the main flow and to diffuse across the cell. If the height of the main reservoir was greater than the injection reservoir, there would be no driving force for material from the injection reservoir to enter the cell and, hence, no material would be detected. Alternatively, if the injection reservoir had a greater head height, material would be forced into the main carrier flow and, hence, could seriously disrupt the main carrier flow. The two reservoirs are maintained at the same height throughout an experiment via a series of siphons. The two reservoirs are connected via a third reservoir designed to prevent injection solution from entering the carrier reservoir or *vice versa*. Owing to the greater amount of carrier consumed during an experiment, the volume of solution in the 250 mL carrier reservoir was maintained constant via a siphon connection to a 2000 mL volumetric flask.

The flow cell used for the flow injection experiments is shown in Figure 1b. The slit through which the injection solution entered was located in the base of the channel unit, which was otherwise the same as a normal channel unit.[2−6] The detector electrode was located on the coverplate, and hence, the geometry of the cell was similar to the double channel electrode where the generator and detector electrodes were on opposite walls of the channel. Thus, detection of material that entered at the slit required the main convective flow to be slow enough to allow diffusion across the channel before the species of interest is swept past the detector electrode.

The injection was controlled by altering the flow rate by switching between different bore flow capillaries connected to a Hamilton valve. At fast flow rates no injection material reaches the far wall before being swept out of the channel, and hence, the injection is "off". Decreasing the flow rate results in injection material reaching the far wall, and thus, the injection is switched "on". Hence, in this way injection solution is always entering the channel and there is no requirement for a mechanical switching mechanism within the vicinity of the cell. The method of adjusting the flow rate to turn the injection on and off was used because a switching mechanism, which involved blocking and unblocking the injection flow line before the cell (via a tap or valve), would leave injection material still in the injection slit between the tap and the channel. While the valve was in the off position, injection solution would continue to diffuse into the cell. Thus, the concentration of injection solution near the surface of the slit would be slowly reduced. When the injection is switched on, the buildup of the transient would be influenced by the amount of dilution near the slit entrance. Since the amount of dilution would be dependent on the time the injection flow stream had been turned off, the buildup of the transient would also be dependent on this time.

Solution that leaves the injection flow cell passes into a section of tubing with the internal diameter alternating between 1.5 and 2 mm every 5 mm for 10 steps. The function of this tubing was to thoroughly mix the injection and carrier solutions prior to entering the second channel flow cell downstream of the injection cell. The purpose of the second cell was to measure the bulk concentration of the injected species in the main carrier flow so that the flux of material entering the main flow from the injection slit could be determined.

With the dual flow system used for the flow injection channel flow cell (shown in Figure 2) the reference electrode was positioned upstream of the cells and the counter electrode downstream. The flow system was constructed from Pyrex tubing joined with B5 ground glass cone and socket joints with wax as a sealant. The reference electrode was a Silver wire "pseudoreference", and the counter electrode consisted of 52 mesh platinum gauze (Goodfellows, Cambridge, UK). The injection flow line was constructed of a 0.2 mm bore glass capillary joined to a 100 cm^3 reservoir. The capillary was attached to the reservoir and to the injection slit in the flow cell with small sections of silicone rubber tubing. Siphons between reservoirs, used to maintain the injection and carrier reservoirs at the same height, were also made of silicone tubing.

The flow cell was constructed of Perspex. The channel unit had dimensions of 60 mm × 6 mm, and when mated together the cell height ($2h$) was either 0.381 or 0.600 mm in all experiments reported below. The injection slit was located in the base of the channel unit and was machined from a Teflon rod. A 0.2 mm bore hole was drilled through the center of the cylinder. In the end of the rod, which sat flush with the base of the channel unit, a slit of length 0.18 mm was cut using a purpose-built rotating blade. The injection flow line was attached to the external end of the rod. The Teflon slit had a width of 3.67 mm and thus did not stretch across the entire channel.

The coverplate that was mated to the channel unit was made of Perspex. The electrodes were cut from platinum foil (Goodfellows, Cambridge, UK) and were typically 4 mm × 4 mm with a thin adjoining tail. The tail provided a means for electrical connection by being fed through a hole in the coverplate. Araldite epoxy resin was used to cement the electrode onto the inside face of the coverplate and to seal the hole in the coverplate. The cemented electrode was polished

to a smoothness of 0.25 μm using progressively decreasing sizes of a diamond-lapping compound (Engis Ltd. Maidstone, UK).

In the experiments to characterize the cell, the solution in the injection reservoir was 100 mM potassium ferricyanide with a background electrolyte of aqueous 0.2 M KCl/0.1 M KOH. The main carrier solution was aqueous 0.2 M KCl/0.1 M KOH. The viscosities of these solutions were measured using a British standard Ostwald viscometer (BS/UA) according to the standard experimental protocol,[11] and the densities were measured using a 50 cm^3 density weighing bottle. Solutions and the viscometer or density bottle were allowed to thermally equilibrate at 23 °C for 20 min in a water bath prior to measurement.

For the investigation of the dyeing of cotton cloth with orange G the same flow injection channel flow cell was used. The coverplate was modified with a recess to allow the cloth to be positioned flush with the coverplate surface and directly adjacent to the electrode, as described previously.[2] The electrode was constructed from copper plated with mercury according to the protocol of Daly *et al.*[12] Flowing through the main carrier flow system was an aqueous solution with a background electrolyte of 0.1 M NaCl, 0.0275 M KH_2PO_4, and 0.0275 M Na_2HPO_4. The injection solution was 50 mM orange G in an aqueous background of 0.1 M NaCl, 0.0275 M KH_2PO_4, and 0.0275 M Na_2HPO_4. The orthophosphate buffer solution maintained the solution pH constant at 6.8 over the length of the experiment. At this pH the voltammetry of the azo linkage gave a single four-electron reduction wave:[13]

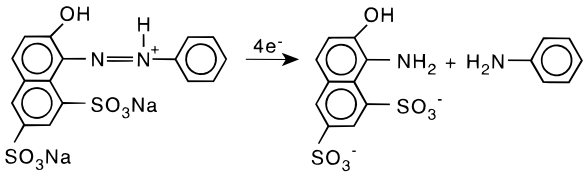

In a typical experiment carrier solution was flowed through the cell for at least 20 min before the flow rate was reduced to allow exposure of the cloth to the dye. Between dyeing experiments the cloth was flushed clear of dye by flowing the carrier solution through the cell for at least 20 min after there was no longer any visible sign of dye on the cloth. This procedure gave reproducible dyeing transients. To compare the injection current when the cloth was present to when the cloth was absent, the cell was dismantled after all the dyeing runs were completed and the coverplate reversed so that the electrode was upstream of the cloth. The cell was reassembled with the identical gap between the injection slit and electrode, and the cell height was confirmed to be unchanged.

The channel flow cell was air thermostated in a Perspex box at 35.5 ± 0.5 °C for all dyeing experiments. All solutions were degassed with argon for at least 20 min before an experiment. Cell height calibrations were conducted at 25 °C with a 1 mM fluorescein solution with a background electrolyte of 0.1 M KOH. Fluorescein has a reported diffusion coefficient of 3.2 × 10^{-6} cm^2 s^{-1} at 25 °C.[14] The cell height was calculated using the Levich equation for a channel flow cell.[15] Potassium ferricyanide, potassium chloride, potassium hydroxide, potassium dihydrogen orthophosphate, disodium hydrogen orthophosphate, and sodium chloride were all AnalaR and obtained from BDH (Poole, UK). The orange G was supplied by Zeneca Fine Chemicals (Manchester, UK), and the fluorescein was from Aldrich (Dorset, UK). All solutions were made using Elgastat (High Wycombe, UK) UHQ grade water outgassed with argon. The cloth used was scoured/bleached unmercerised flat-woven indian head cotton supplied by Zeneca Specialties (Manchester, UK).

Results and Discussion

Solution Characteristics. Before injection experiments were conducted, the density and viscosity of the injection solution and the main carrier solution were measured, since significant differences between the solutions might result in quite different injection results. The viscosity and density of the injection solution, 100 mM potassium ferricyanide in water with a background electrolyte of 0.2 M KCl and 0.1 M KOH, were 0.946 ± 0.001 cP and 1.027 ± 0.001 g cm^{-3}, respectively. For the carrier solution, 0.2 M KCl and 0.1 M KOH in water, they were 0.932 ± 0.001 cP and 1.010 ± 0.001 g cm^{-3}. Note that to ascertain the reliability of the measurements, the viscosity and density of water were also measured as 0.932 ± 0.001 cP and 0.997 ± 0.001 g cm^{-3}, respectively, which compares well with the literature values[16] at 23 °C of 0.9310 cP and 0.997 g cm^{-3}. The diffusion coefficient of the ferricyanide solution assumed was the reported literature value of 7.6 × 10^{-6} cm^2 s^{-1} in 0.2 M KCl.[17]

Effect of the Injection on the Carrier Flow. The flow rates of the three main flow capillaries were calibrated from the volume of solution emerging from the flow system with the cell separated from the injection flow line. These flow rates were compared to the measured flow rate when the injection line was attached to the injection cell and injection material was entering the cell via the injection slit. For a given head height, Δh, and capillary, the flow rate was found to be the same whether the injection stream was on or off, which confirmed that there was only minor flow of injection solution into the flow cell. Unless otherwise indicated, the flow rates quoted throughout this paper are those determined from the volume of solution leaving the flow system with time when the injection solution was entering the cell.

To confirm that the flow of injection solution was not causing significant disruption to the main carrier flow, *both* the injection reservoir and the carrier reservoir contained 8.1 mM potassium ferricyanide in water with a background electrolyte of 0.2 M KCl and 0.1 M KOH. The cell dimensions used were electrode width = 0.405 cm, electrode length = 0.423 cm, and the gap between the slit and electrode was 1.200 cm. The steady-state current was measured at a variety of flow rates with the injection flow line attached and compared to that obtained when no injection material was entering the channel. In both configurations the dependence of the limiting current on flow rate conformed to the Levich equation[15] for the channel flow cell,

$$I_{\mathrm{lim}} = 0.925nFwc_{\infty}\left[\frac{V_f D^2 x_e^{\,2}}{h^2 d}\right]^{1/3} \qquad (1)$$

where I_{lim} is the limiting current, n is the number of electrons transferred, F is the Faraday constant, c_∞ is the bulk concentration, w is the electrode width, V_f is the volume flow rate, D is the diffusion coefficient, x_e is the electrode length, h is the cell half height, and d is the channel width.

The plot of I_{lim} vs $V_f^{1/3}$ when injection material was entering the channel was linear and identical within experimental error to the case where no material was entering the cell via the injection slit. It was concluded, therefore, that the injection of material into the cell by this method did not significantly affect the primary channel flow profile. This conclusion is supported by the theoretical analysis of the flow injection channel flow cell.[1]

Influence of the Main Carrier Flow on the Flux of Material from the Injection Slit. When background solution is flowing through the primary channel and injection solution is entering from the injection line, the magnitude of the current

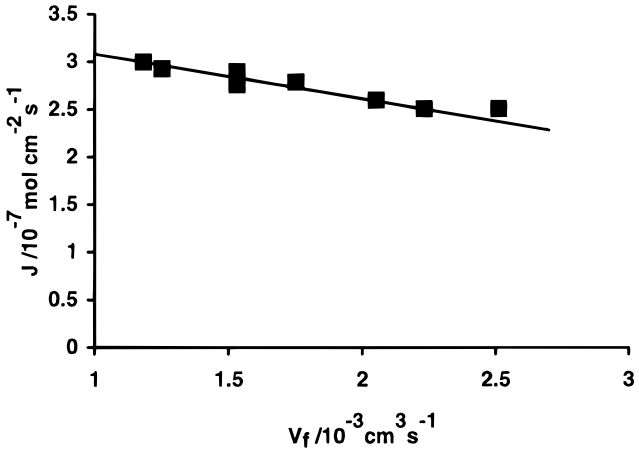

Figure 3. Variation in flux of injection solution into the channel with flow rate for a flow injection channel flow cell of the following dimensions: cell height = 0.0381 cm, cell width = 0.600 cm, slit length = 0.018 cm, and slit width = 0.367 cm.

recorded at the detector electrode, the injection current, for a given flow rate is dependent on the flux of injection solution entering the cell. To determine how much injection material was entering the main flow stream from the injection slit, the second flow cell in the flow system (see Figure 2) was used. The flow system was set up for an injection experiment with aqueous 0.2 M KCl/0.1 M KOH solution flowing through the carrier flow line and an aqueous solution of 100 mM potassium ferricyanide and 0.2 M KCl/0.1 M KOH entering the cell via the injection slit. The solution leaving the injection cell thus contained an inhomogeneous mixture of injection and carrier solutions. As the solution passed through a section of tubing of constantly changing diameter, the ferricyanide and carrier solutions were mixed before entering the calibration flow cell. The current measured in the calibration cell enabled the calculation of the concentration of injection solution in this homogeneous mixture. After an injection transient was recorded, the flow rate was held at the injection flow rate. The calibration cell current was monitored until it became constant. The current from the calibration cell was converted to a flux from the slit as follows. The bulk concentration of injection species in the main carrier stream, c_∞, was calculated using the Levich equation[15] (eq 1) for a channel flow cell. From this concentration the average flux from the slit could be determined using

$$J = \frac{c_\infty V_f}{A} \qquad (2)$$

where J is the flux and A is the area of the slit.

The variation in the flux with flow rate is shown in Figure 3 for the flow injection channel flow cell with dimensions $2h$ = 0.0381 cm, channel width = 0.600 cm, slit width = 0.367 cm, and slit length = 0.018 cm. As can be seen from the figure, there is a small but constant variation in flux with flow rate. This variation in flux with flow rate is attributed to changes in the disturbances of the laminar flow in the region of the slit as the flow rate is increased, as was illustrated with the FLOTRAN modeling of the flow injection channel flow cell.[1] When solution flows past an inlet, a low-pressure region is produced adjacent to the leading edge of the inlet and there will be some disturbance in the solution. The form of this disturbance, and its influence on material entering the main flow stream, is dependent on a variety of variables including the flow rate, the shape of the inlet, and the solution viscosity. The solution flow

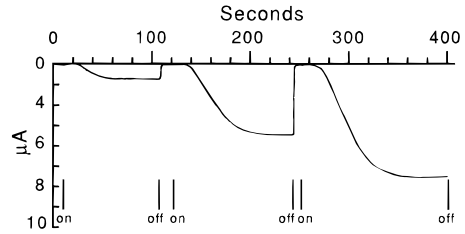

Figure 4. Flow injection transients for flow rates 2.14×10^{-3}, 1.53×10^{-3}, and 1.32×10^{-3} cm^3 s^{-1}. Cell dimensions are as in Figure 4 except gap length = 1.037 cm, electrode length = 0.395 cm, and electrode width = 0.401 cm.

TABLE 1: Cell Dimensions for Flow Injection Results Presented in Figures 5−7[a]

data set	slit length	slit width	gap length	electrode length	electrode width	cell height
1	0.018	0.367	1.204	0.395	0.419	0.0381
2	0.018	0.367	0.376	0.432	0.388	0.0381
3	0.018	0.367	1.298	0.432	0.388	0.0381
4	0.007	0.600	1.839	0.283	0.285	0.0600

[a] All dimensions are in centimeters.

in the flow injection cell and its effect on the flux of injection solution into the cell are discussed elsewhere.[1]

Transients Observed with the Flow Injection Cell. As discussed in the Experimental Section, the injection in the channel was switched on and off by adjusting the flow rate between fast and slow flow rates. Three transients using this method are shown in Figure 4. The cell dimensions for these transients were gap length = 1.037 cm, electrode length = 0.395 cm, and electrode width = 0.401 cm. The fast flow rate (corresponding to "no injection", since all the injection material is swept out of the channel before it can diffuse to the far wall of the channel) was greater than 10^{-2} cm^3 s^{-1}, and the flow rates for the three transients were 2.14×10^{-3} cm^3 s^{-1}, 1.53×10^{-3} cm^3 s^{-1}, and 1.32×10^{-3} cm^3 s^{-1}, respectively. As expected, the steady-state current value was higher the lower the flow rate, but the time taken to reach steady state was increased. Figure 4 also illustrates how rapidly the injection is turned off by increasing the flow rate. This almost instantaneous turning off of the detector signal is ideal for experiments where only a pulse of injection solution is required, or if the effect after turning off the injection is of interest, as in desorption experiments.

Variation of Injection Current with Flow Rate. The three transients in Figure 4 show that as the main carrier flow is increased, the steady-state detector current is reduced as expected. This variation in steady-state detector current for the flow injection cell with flow rate for different cell dimensions, as shown in Table 1, was measured and compared to the theoretically predicted steady-state currents. A plot of steady-state current vs flow rate is shown in Figure 5 for data set 1. Thus, the solution flow rate in the flow injection cell can be used to control the extent to which material entering the flow cell can reach the opposite side and react with the solid substrate. The dramatic increase in the amount of injection material that reaches the far wall of the channel with a minor reduction in flow rate, especially at low flow rates, would enable the investigation of an interfacial process over a wide range of reactant conditions and hence reaction rates.

The influence of the gap length on the measured injection current is shown in parts a and b of Figure 6 for data sets 2 and 3, respectively, where the same electrode and channel dimensions are used for two different gap lengths of 0.376 and 1.298 cm. The figure clearly shows a large decrease in the current

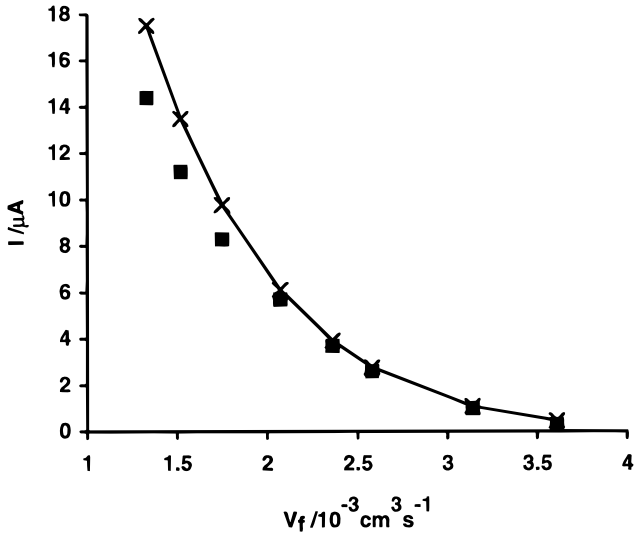

Figure 5. Comparison between the steady-state injection current measured experimentally (■) and predicted by the BIFD flux model (full line and ×) for data set 1. See Table 1.

monitored at the detector electrode with a decrease in the gap length. In relative terms this decrease with gap length is much greater at higher flow rates. One advantage with decreasing the gap length is that the smaller the gap between the injection slit and the detector electrode, the shorter is the time taken for the injection transient to reach steady state.

Comparison between Theoretical and Experimental Results. The steady-state currents predicted by the BIFD flux model[1] were compared to flow injection results for cells of dimensions as shown in Table 1. The predicted currents using FLOTRAN[1] are also shown where calculated. The flux incorporated into the programs was derived from the calibration current determined from the second downstream channel flow cell.

The comparison between theory and experiment is shown in Figures 5 and 6. As can be seen from the figures, there is good agreement between theory and experimental results. This agreement is particularly impressive when it is considered that no adjustable parameters have been used in the modeling methods. Parts a and b of Figure 6 show that there is close agreement between the currents predicted by BIFD and by FLOTRAN, but identity should not be expected. The assumptions made in using the BIFD method (constant parabolic laminar flow throughout the channel; slit represented as a flux input boundary condition) were shown to be satisfactory approximations[1] but are of course not identical with the conditions being solved by FLOTRAN. For the longer gap (1.298 mm) between slit and electrode with theoretical currents up to 24 μA, BIFD is slightly higher than FLOTRAN by 0.9−1.2 μA at the slower flow rates but lower by 0.3 μA at the fast flow rate. For the short gap (0.367 mm) with currents up to 5 μA, BIFD varies from 0.166 μA higher to 0.147 μA lower than FLOTRAN.

Figures 5 and 6 show that the agreement between experimental and theoretical currents is particularly good at fast flow rates, but as the flow rate decreases, the experimental values begin to diverge with the experimentally determined current falling below the predicted values. The difference is more marked for the data in Figure 6, for which a narrower detector electrode was used than for the data in Figure 5. It was hypothesized that the deviation between the model and experimental data at slower flow rates was due to some degree of lateral diffusion in the *z*-direction in the flow injection channel.

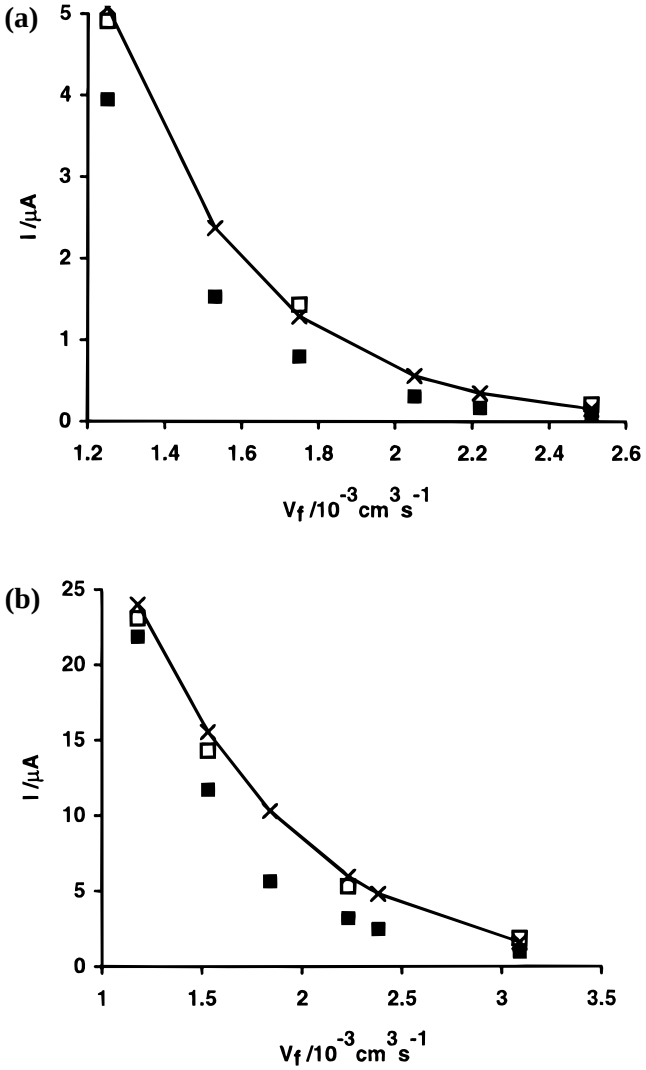

Figure 6. Comparison between the steady-state injection current measured experimentally (■) predicted by the BIFD flux model (full line and ×) and FLOTRAN (□) for (a) data set 2 and (b) data set 3. See Table 1.

With the Teflon injection slit used for data sets 1−3 the slit width was only 0.367 cm while the channel width was 0.600 cm. Thus, with the longer gap lengths and slower flow rates there is more time for material that enters the cell from the slit to diffuse toward the side walls. It should be noted that both the BIFD approach and the FLOTRAN model calculated a two-dimensional solution. Considering that material has time to diffuse across the channel from the slit to the detector electrode, it seems likely that some will be lost owing to diffusion in the *z*-direction.

The hypothesis was tested by building a new cell with a slit that extended across the whole channel. The comparison between the experimental results for the wider slit, with dimensions as in Table 1 for data set 4, and the predicted current variation with the flow rate using the BIFD flux model is shown in Figure 7. As can be seen from Figure 7, the experimental and theoretical currents do not appear to be systematically diverging as was observed with data sets 1−3 with the narrower slit.

The problem of diffusion in the *z*-direction could also be addressed in other ways. FLOTRAN has the capability of using a three-dimensional finite element grid. However, the time involved in running this program may be substantial. An alternative would be to make the width of the detector electrode

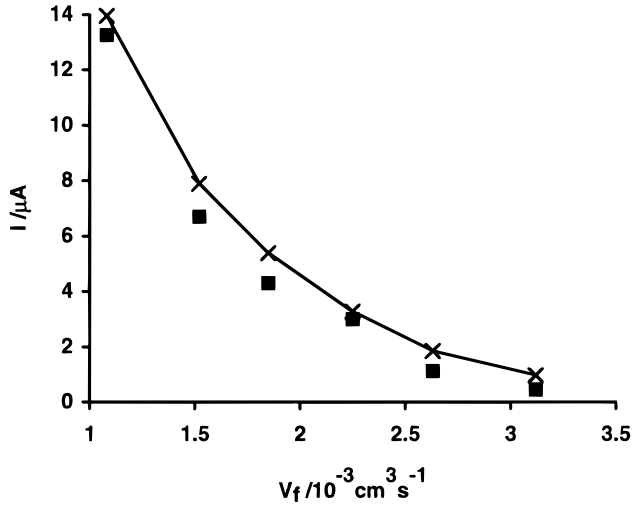

Figure 7. Comparison between the steady-state injection current measured experimentally (■) and predicted by the BIFD flux model (full line and ×) for data set 4 where the injection slit was across the whole channel. See Table 1.

small relative to the injection slit. Such a method has already received preliminary attention with the wider injection slit stretched all the way across the channel. Recent developments with microelectrodes in channel flow cells[18,19] suggest that using microelectrode detectors is another possibility.

Investigation of a Solid/Solution Interfacial Reaction Using the Flow Injection Channel Flow Cell. The ability to interrogate the surface with very small amounts of injection solution is particularly useful for investigating rapid reactions. If the solid substrate is quickly exposed to a large concentration of the species of interest, the transient response will be very rapid as the surface becomes swamped with reactant. With the presently employed geometry the flow rate can be selected so that even at steady state very little reactant reaches the surface, giving a much improved method for the quantification of the interfacial kinetics.

The reaction between the model dye, orange G, and cotton cloth has been investigated previously using a conventional channel flow cell.[2] It was shown that at slow flow rates there was no flux of dye into the cloth. It was proposed that this lack of dyeing was due to the blocking of channels within the porous surface layer through which the dye must travel to penetrate the bulk cloth. To gain information pertaining to the initial transport and then the blocking of the surface layer requires the use of the flow injection channel flow cell. With this cell, dye-free cloth can be exposed to dye and the change in flux of material into the cloth monitored with time.

An injection transient, at a flow rate of 1.53×10^{-3} cm^3 s^{-1}, with the cotton cloth present is shown in Figure 8 for a channel where the cell height was 0.0381 cm, the slit length was 0.018 cm, the gap length was 0.529 cm, cloth length was 0.420 cm, electrode length was 0.386 cm, and electrode width was 0.400 cm. Also shown in Figure 8 is a transient where there is no cloth present. All cell dimensions are the same except that the gap length is 0.949 cm to compensate for the absence of the cloth. Comparison of the two transients shows several interesting features. First, there is the obvious difference in steady-state current, which is attributed to loss of dye due to dyeing of the cloth. Second, the time for the initial rise in current due to injection material reaching the electrode is similar as would be expected for the same distance between injection slit and the detector electrode. However, when the cloth is present there is a plateau before beginning to increase more rapidly. In the absence of the cloth there is no such plateau. It is proposed

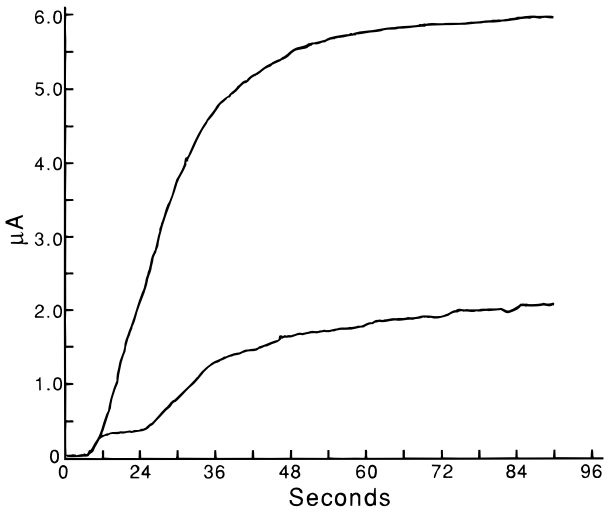

Figure 8. Injection transients for a flow rate of 1.53×10^{-3} cm^3 s^{-1} of orange G in the presence of cotton cloth (lower transient) and in the absence of cloth. The gap between the electrode of dimensions 0.386 cm × 0.400 cm was 0.949 cm. In the presence of the cloth this gap comprised 0.529 cm of inert surface and 0.42 cm of cotton directly adjacent to the electrode.

that the plateau is due to a large portion of the dye that first reaches the cloth being adsorbed onto the surface layer. Once these surface sites are filled, dye must undergo the slower process of diffusing from the surface layer into the bulk cloth, and thus, the transient begins to rise again. Finally, although the injection transient appears to settle to a steady value, the current continues to increase slowly with time and was observed to do so for more than 1 h. This slow increase in current with time is attributed to the porous channels through the surface layer of the cotton cloth becoming blocked, which is in agreement with the previously proposed mechanism for the dyeing of cotton with orange G.[2]

This initial example of the use of the flow injection channel flow cell for the investigation of rapid heterogeneous reactions illustrates how evidence for proposed reaction mechanisms can be derived even prior to detailed theoretical analysis of the injection behavior of the reaction.

Conclusions

The flow injection cell designed allows any solution species to be introduced into a channel flow cell at a defined time for a defined time period. When the injection is turned off, the detector current dies away to zero within a couple of seconds, thus giving the cell the potential to be used in the investigation of desorption experiments. The location of the injection slit in the wall of the channel opposite the detector electrode and the solid substrate of interest has distinct advantages in investigating heterogeneous reaction kinetics, especially for rapid reactions.

Excellent agreement between experimentally measured steady-state injection currents and those predicted using the BIFD flux model indicates that there is little disruption of the well-defined flow in a conventional channel flow cell. The application of the flow injection cell to the investigation of processes at solid liquid interfaces was demonstrated with a preliminary study of the dyeing of cotton cloth by the dye orange G.

Acknowledgment. We thank Zeneca for support. J.J.G. thanks Merton College, Oxford, for a Senior Scholarship.

References and Notes

(1) Gooding, J. J.; Coles, B. A.; Compton, R. G. *J. Phys Chem.* **1997**, *101*, 175.

(2) Gooding, J. J.; Compton, R. G.; Brennan, C. M.; Atherton, J. H. *J. Colloid Interface Sci.*, in press.

(3) Compton, R. G.; Harding, M. S.; Atherton, J. H.; Brennan, C. M. *J. Phys. Chem.* **1993**, *97*, 4677.

(4) Compton, R. G.; Unwin, P. R. *Compr. Chem. Kinet.* **1989**, *29*, 173.

(5) Compton, R. G.; Harding, M. S.; Pluck, M. R.; Atherton, J. H.; Brennan, C. M. *J. Phys. Chem.* **1993**, *97*, 10416.

(6) Compton, R. G.; Sanders, G. H. W. *J. Colloid Interface Sci.* **1993**, *158*, 439.

(7) *Flotran Theoretical Manual*; ANSYS Inc.: Houston, PA, 1992.

(8) Compton, R. G.; Coles, B. A.; Fisher, A. C. *J. Phys. Chem.* **1994**, *98*, 2441.

(9) Compton, R. G.; Pilkington, M. B. G.; Stearn, G. M. *J. Chem. Soc., Faraday Trans. 1* **1988**, *84*, 2155.

(10) Anderson, J. L.; Moldoveanu, S. *J. Electroanal. Chem.* **1984**, *179*, 107.

(11) Levitt, B. P., Ed.; *Findlay's Practical Physical Chemistry;* Longman: London, 1973.

(12) Daly, P. J.; Page, D. J.; Compton, R. G. *Anal. Chem.* **1983**, *55*, 1191.

(13) Gooding, J. J.; Compton, R. G.; Brennan, C. M.; Atherton, J. H. *Electroanalysis (N.Y.)*, in press.

(14) Coles, B. A.; Compton, R. G. *J. Electroanal. Chem.* **1983**, *144*, 87.

(15) Levich, V. G. *Physicochemical Hydrodynamics*; Prentice Hall: Englewood Cliffs, NJ, 1962.

(16) Dean, J. A., Ed.; *Lange's Handbook of Chemistry*; McGraw and Hill: New York, 1985.

(17) Von Stackelberg, M. V.; Pilgram, M.; Toome, V. *Z. Elektrochem.* **1953**, *57*, 342.

(18) Compton, R. G.; Fisher, A. C.; Wellington, R. G.; Dobson, P. J.; Leigh, P. A. *J. Phys. Chem.* **1993**, *97*, 10410.

(19) Booth, J.; Compton, R. G.; Cooper, J. A.; Dryfe, R. A. W.; Fisher, A. C.; Davies, C. L.; Walters, M. K. *J. Phys. Chem.* **1995**, *99*, 10942.